

# Kinetics and Mechanism of the Initial Phase of the Bromine–Chlorite Ion Reaction in Aqueous Solution

Zsuzsanna Tóth and István Fábián\*

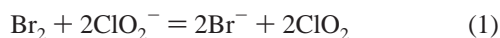
Department of Inorganic and Analytical Chemistry, University of Debrecen, P.O.B. 21, Debrecen H-4010 Hungary

Received March 23, 1999

The kinetics and mechanism of the chlorine(III)–bromine reaction are studied by the stopped-flow method under acidic conditions in 1.0 M NaClO<sub>4</sub> and at 25.0 °C. There are two kinetically well-separated phases in this reaction. A detailed mechanism is proposed for the first phase of the reaction, in which Br<sub>2</sub> oxidizes ClO<sub>2</sub><sup>−</sup> to chlorine dioxide. It is confirmed that the oxidation occurs via competing parallel reaction steps. The autoinhibition observed in the reaction is attributed to a backward shift in the reversible initial step as the oxidation proceeds. On the basis of simultaneous evaluations of the kinetic traces, the following forward rate constants are obtained for the kinetically significant reaction steps: Br<sub>2</sub> + ClO<sub>2</sub><sup>−</sup> ⇌ ClO<sub>2</sub> + Br<sub>2</sub><sup>−</sup>,  $k_1 = (1.3 \pm 0.2) \times 10^3 \text{ M}^{-1} \text{ s}^{-1}$  ( $k_{-1} = 1.1 \times 10^9 \text{ M}^{-1} \text{ s}^{-1}$ ); Br<sub>2</sub><sup>−</sup> + ClO<sub>2</sub><sup>−</sup> = ClO<sub>2</sub> + 2Br<sup>−</sup>,  $k_2 = (4.0 \pm 0.1) \times 10^6 \text{ M}^{-1} \text{ s}^{-1}$ ; Br + ClO<sub>2</sub><sup>−</sup> = ClO<sub>2</sub> + Br<sup>−</sup>,  $k_8 = (2.3 \pm 0.7) \times 10^8 \text{ M}^{-1} \text{ s}^{-1}$ ; HOBr + HClO<sub>2</sub> = BrClO<sub>2</sub> + H<sub>2</sub>O (BrClO<sub>2</sub> + ClO<sub>2</sub><sup>−</sup> = Br<sup>−</sup> + 2ClO<sub>2</sub>, very fast),  $k_9 = (1.9 \pm 0.1) \times 10^5 \text{ M}^{-1} \text{ s}^{-1}$ . The possible kinetic role of the reactive BrClO<sub>2</sub> intermediate is discussed in detail.

## Introduction

The kinetics and mechanisms of chlorine dioxide formation in the bromine–chlorite ion system were previously studied by Valdes-Aguilera and co-workers.<sup>1</sup> The reaction was characterized with a strictly 1:2 final stoichiometry:



According to these authors, simple first-order kinetic traces were observed whenever the chlorite ion was used in excess over Br<sub>2</sub>. The appropriate rate law was deduced on the basis of the concentration dependencies of the pseudo-first-order rate constants.

The reactions of the chlorite ion are notorious for their complexities, and the relatively simple stoichiometric and kinetic features reported for this system are somewhat unexpected. The most interesting result from the cited paper is the direct observation of the BrClO<sub>2</sub> intermediate. The first X<sub>2</sub>O<sub>2</sub>-type transient species (X = halogen atom) was postulated in 1948 by Taube and Dodgen<sup>2</sup> in their study of the reactions of the chlorite ion with Cl<sub>2</sub> and HOCl. Since then, the formation and subsequent reactions of these reactive intermediates have been in the cores of the mechanisms postulated for aqueous reactions of oxyhalogen species.<sup>3–15</sup> Some of the X<sub>2</sub>O<sub>2</sub> species were

detected in polycrystalline ice and gas phases, and theoretical discussions of their structures and reactivities were presented.<sup>16–23</sup> However, direct experimental evidence to prove the existence of such species in aqueous solutions has not, until now, been found. The primary objective of our present study was to obtain evidence for the formation of BrClO<sub>2</sub> and, if possible, to observe its properties in selected reactions. Because BrClO<sub>2</sub> can be considered as a prototype of the X<sub>2</sub>O<sub>2</sub> intermediates, the results were also expected to lead to a better understanding of the significance of these species in the redox chemistry of oxyhalogen compounds.

Our preliminary experiments were not fully consistent with the results reported by Valdes-Aguilera and co-workers.<sup>1</sup> We found no direct experimental evidence for the formation of BrClO<sub>2</sub>, and most of our kinetic traces showed significant

\* Corresponding author. E-mail: ifabian@delfin.klte.hu.

- (1) Valdes-Aguilera, O.; Boyd, D. W.; Epstein, I. R.; Kustin, K. *J. Phys. Chem.* **1986**, *90*, 6696–6702.
- (2) Taube, H.; Dodgen, H. *J. Am. Chem. Soc.* **1949**, *71*, 3330–3336.
- (3) Emmenegger, F.; Gordon, G. *Inorg. Chem.* **1967**, *6*, 633–635.
- (4) Gordon, G.; Kieffer, R. G.; Rosenblatt, D. H. *Prog. Inorg. Chem.* **1972**, *15*, 201–286.
- (5) Grant, J. L.; De Kepper, P.; Epstein, I. R.; Kustin, K.; Orbán, M. *Inorg. Chem.* **1982**, *21*, 2192–2196.
- (6) Tang, T.; Gordon, G. *Environ. Sci. Technol.* **1984**, *18*, 212–216.
- (7) Epstein, I. R.; Kustin, K. *J. Phys. Chem.* **1985**, *89*, 2275–2282.
- (8) Aieta, E. M.; Roberts, P. V. *Environ. Sci. Technol.* **1986**, *20*, 50–55.

- (9) Rábai, G.; Beck, M. T. *Inorg. Chem.* **1987**, *26*, 1195–1199.
- (10) Peintler, G.; Nagypál, I.; Epstein, I. R. *J. Phys. Chem.* **1990**, *94*, 2954–2958.
- (11) Gordon, G.; Tachiyashiki, S. *Environ. Sci. Technol.* **1991**, *25*, 468–474.
- (12) Fábián, I.; Gordon, G. *Inorg. Chem.* **1992**, *31*, 2144–2150.
- (13) Rábai, G.; Orbán, M. *J. Phys. Chem.* **1993**, *97*, 5935–5939.
- (14) Furman, C. S.; Margerum, D. W. *Inorg. Chem.* **1998**, *37*, 4321–4327.
- (15) Xie, Y.; McDonald, M.; Margerum, D. W. *Inorg. Chem.* **1999**, *38*, 3938–3940.
- (16) Müller, H. S. P.; Willner, H. *Ber. Bunsen-Ges. Phys. Chem.* **1992**, *96*, 427–431.
- (17) Müller, H. S. P.; Willner, H. *Inorg. Chem.* **1992**, *31*, 2527–2534.
- (18) Jacobs, J.; Kronberg, M.; Müller, H. S. P.; Willner, H. *J. Am. Chem. Soc.* **1994**, *116*, 1106–1114.
- (19) Francisco, J. S.; Sander, S. P. *J. Am. Chem. Soc.* **1995**, *117*, 9917–9918.
- (20) Johnson, K.; Engdahl, A.; Kölm, J.; Nieminen, J.; Nelander, B. *J. Phys. Chem.* **1995**, *99*, 3902–3904.
- (21) Pursell, C. J.; Conyers, J.; Denison, C. *J. Phys. Chem.* **1996**, *100*, 15450–15453.
- (22) Guha, S.; Francisco, J. S. *J. Phys. Chem. A* **1997**, *101*, 5347–5359.
- (23) Misra, A.; Marshall, P. *J. Chem. Soc., Faraday Trans.* **1997**, *93*, 3301–3304.

deviations from pseudo-first-order behavior. In the present study, the kinetics of the oxidation of the chlorite ion by bromine is reinvestigated. On the basis of a new set of experimental data, we propose an improved mechanism which seems to be consistent with our observations. While this work was in progress, a thorough kinetic study of the related  $\text{HOBr}-\text{ClO}_2^-$  reaction under slightly acidic–neutral conditions was published by Furman and Margerum.<sup>14</sup> The results reported by these authors and those obtained here are complementary and are used to provide a detailed interpretation of the  $\text{Br}_2/\text{HOBr}-\text{ClO}_2^-/\text{HClO}_2$  reaction over an extended pH range.

## Experimental Section

**Chemicals.** Commercially available  $\text{NaClO}_2$  (Fluka, 80% purity) was purified as described earlier.<sup>24</sup> Bromine stock solutions were prepared by distilling  $\text{Br}_2$  (Ferah) into 0.01 M  $\text{HClO}_4$  (Carlo Erba) solution.<sup>25</sup> The ionic strength was adjusted to 1.00 M with  $\text{NaClO}_4$  prepared from perchloric acid (Carlo Erba) and  $\text{Na}_2\text{CO}_3$  (Reanal). All other reagents were of analytical grade and were used without further purification. The reagent solutions were prepared in doubly deionized and ultra-filtered water obtained from a Milli-Q RG (Millipore) water purification system. pHs were calculated from the total concentrations of the components by using the appropriate equilibrium constants for the pH-dependent equilibrium steps. pH corresponds to  $-\log [\text{H}^+]$  throughout this paper. With a few exceptions, all experiments were carried out by using a large excess of the chlorite ion over bromine.

**Instrumentation and Methods.** Bromine stock solutions were stored in and dispensed from a home-built, electronic version of the “shrinking bottle” described by Silverman and Gordon.<sup>26</sup> With this device, bromine solutions could be stored with less than 1% concentration loss per day and the error of each dispensed volume was  $\pm 0.5\%$ . The concentrations of  $\text{Br}_2$  were determined by the standard iodometric method using a Metrohm 721 NET Titrimetric potentiometric titrator equipped with a Metrohm combined platinum wire electrode.

Spectrophotometric measurements were performed with an HP-8453 spectrophotometer, and kinetic measurements were obtained with an Applied Photophysics DX-17 MV sequential stopped-flow apparatus either in the single-wavelength detection mode or by using an Applied Photophysics PDA 1 diode array detector. At longer reaction times, time-resolved spectra were recorded on the HP-8453 spectrophotometer equipped with an RX2000 Rapid Kinetics Spectrometer Accessory (Applied Photophysics). The optical path was 10 mm, and all measurements were made at  $25.0 \pm 0.1$  °C. The kinetic runs were triggered by mixing acidic bromine and neutral chlorite ion solutions in 1:1 ratios. In the corresponding experiments,  $\text{Br}^-$  was added to the bromine solution. The individual stopped-flow traces were fitted with the program package SCIENTIST.<sup>27</sup> For simultaneous evaluations of more than one kinetic curve, the program package ZITA was used.<sup>28</sup>

**Equilibrium Constant for the  $\text{Br}_2 + \text{Br}^- \rightleftharpoons \text{Br}_3^-$  Reaction.** This equilibrium constant was redetermined spectrophotometrically for the conditions applied here. The individual samples were prepared by adding excess  $\text{NaBr}$  to  $\text{NaBrO}_3$  solutions in increasing concentrations at pH 1.00.<sup>29</sup> Prior to spectral acquisitions at 25.0 °C, the samples were incubated at 50 °C in sealed vials for 3 h. Under these conditions, the bromate ion was completely converted to  $\text{Br}_2$ . The equilibrium constant and the molar absorptivities of  $\text{Br}_2$  and  $\text{Br}_3^-$  at several wavelengths were calculated by using a nonlinear least-squares fitting routine. The

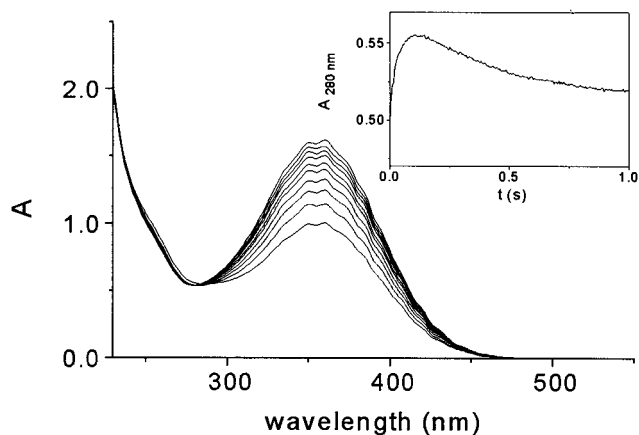


**Figure 1.** Time-resolved spectral changes in the bromine–chlorite ion reaction in the absence of added bromide ion.  $[\text{ClO}_2^-]_0 = 0.01$  M;  $[\text{Br}_2]_0 = 5.0 \times 10^{-4}$  M; pH = 1.50. In the order of increasing absorbance at 360 nm, the spectra were recorded at 0.34, 2.34, 65.9, 237, 457, 599, 786, 901, 1033, and 1185 s. Inset: Stopped-flow trace under the same conditions at 280 nm.

equilibrium constant obtained,  $K = 19.3 \pm 1.2 \text{ M}^{-1}$ , was in excellent agreement with previous literature data.<sup>29–31</sup>

## Results and Discussions

**Preliminary Observations.** Typical time-resolved UV–vis spectra recorded in the absence of added bromide ion indicate composite kinetic features in the  $\text{Br}_2-\text{ClO}_2^-$  system (Figure 1). In the near-UV–visible region, the main absorbing species is  $\text{ClO}_2$  ( $\lambda_{\text{max}} = 360$  nm,  $\epsilon = 1250 \text{ M}^{-1} \text{ cm}^{-1}$ ),<sup>32</sup> while, below 300 nm, the absorbance is due to chlorite ion/chlorous acid,<sup>33</sup>  $\text{ClO}_2$ ,  $\text{Br}_2$ , and  $\text{Br}_3^-$ . A very intense absorbance band is characteristic for  $\text{Br}_3^-$  ( $\lambda_{\text{max}} = 266$  nm,  $\epsilon = 40\,900 \text{ M}^{-1} \text{ cm}^{-1}$ ),<sup>29</sup> which suppresses any spectral effect when the tribromide ion and the other absorbing species are present in comparable concentrations. It should be kept in mind that the contribution of  $\text{Br}_3^-$  to the spectra can be significant even when it is formed at relatively low concentration levels.

As shown, the intensity of the characteristic 360 nm band of  $\text{ClO}_2$  steadily increased in the absence of added bromide ion. At the same time, a very small opposite change was observed in the 260–290 nm region. However, in a few cases, stopped-flow measurements at 280 nm revealed a small absorbance increase at the very beginning of the reaction (Figure 1, inset). These observations can be interpreted as follows. Chlorine dioxide is generated by the oxidation of the chlorite ion, as shown in eq 1. This reaction also produces the bromide ion, which shifts the  $\text{Br}_2-\text{Br}_3^-$  equilibrium toward tribromide ion formation. On the basis of a rough estimate, the small initial absorbance increase at 280 nm corresponds to the conversion of less than 1% of bromine into  $\text{Br}_3^-$ . At longer reaction times (not shown in Figure 1), the absorbance slightly increases again in the UV region. This indicates the formation of  $\text{Br}_2/\text{Br}_3^-$  in a subsequent slow reaction between the excess chlorite ion and  $\text{Br}^-$ .<sup>34</sup>

(24) Fábián, I.; Gordon, G. *Inorg. Chem.* **1991**, *30*, 3785–3787.

(25) Gauw, R. D. Ph.D. Thesis, Miami University, Oxford, OH, 1999.

(26) Silverman, R. A.; Gordon, G. *Anal. Chem.* **1974**, *46*, 178.

(27) SCIENTIST 2.0; Micromath Software: Salt Lake City, UT, 1995.

(28) Peintler, G. *ZITA: A Comprehensive Program Package for Fitting Parameters of Chemical Reaction Mechanisms*; Atila József University: Szeged, Hungary, 1997.

(29) Wang, T. X.; Kelley, M. D.; Cooper, J. N.; Beckwith, R. C.; Margerum, D. W. *Inorg. Chem.* **1994**, *33*, 5872–5878.

(30) Scaife, D. B.; Tyrrell, H. J. V. *J. Chem. Soc.* **1958**, 386–392.

(31) Irving, H.; Wilson, P. D. *J. Inorg. Nucl. Chem.* **1964**, *26*, 2235.

(32) Kieffer, R. G.; Gordon, G. *Inorg. Chem.* **1968**, *7*, 235–239.

(33) In aqueous solutions, the protolytic equilibria between  $\text{HClO}_2$  and  $\text{ClO}_2^-$  are fast and the concentration ratios of the two species are determined by the pH. Unless it has particular significance, we do not distinguish the two species and refer to chlorine(III) as the chlorite ion through this paper.

In the presence of added  $\text{Br}^-$ , the results provided further evidence that there are two kinetically well-separated phases in this reaction. In this case, the  $[\text{Br}_2]/[\text{Br}_3^-]$  ratio was practically constant during the reaction. In the first phase, the fast absorbance change was consistent with the consumption of bromine and the formation of chlorine dioxide. At longer reaction times, the intensity of the characteristic  $\text{Br}_3^-$  band increased because of the formation of  $\text{Br}_2$  in the  $\text{Br}^- - \text{ClO}_2^-$  reaction. The latter process was relatively slow and kinetically coupled with acid-catalyzed decomposition of the chlorite ion. In separate experiments, a similarly slow formation of  $\text{Br}_3^-$  in the  $\text{Br}^- - \text{ClO}_2^-$  reaction confirmed this interpretation.

Our attempt to establish a uniform final stoichiometry for the overall process failed. This is not very surprising because  $\text{Br}_2$  is not only consumed but also generated in the reaction and  $\text{ClO}_2$  is produced by both the oxidation and the acid-catalyzed decomposition of chlorite ion. The actual ratios of the reactants consumed and products formed are determined by the interplay of these reactions and are strongly dependent on the experimental conditions applied. However, in the first phase, when the oxidation of  $\text{Br}^-$  by  $\text{ClO}_2^-$  was negligible, the spectral changes were consistent with the stoichiometry given in eq 1. In the remainder of this paper, kinetic results are presented only for the initial phase of the bromine–chlorite ion reaction. Because of the very intense  $\text{Br}_3^-$  absorbance band at 266 nm, meaningful data could not be collected from the entire UV region in the presence of added bromide ion. Thus, only kinetic traces from the 340–390 nm wavelength region were used for quantitative evaluation of the system.

#### Reaction Orders in the Absence of Added Bromide Ion.

Although a large excess of  $\text{ClO}_2^-$  over  $\text{Br}_2$  was applied, the stopped-flow traces could not be fitted with a single-exponential function in most cases. Because the complexity of the reaction prevented the use of a well-defined, uniform rate law, the reaction orders for the reactants were estimated by using the initial-rate method. This technique is not suitable for exploring the details of a complex reactive system, but it can be efficiently used to establish the basic kinetic features of the reaction. The kinetic traces were fitted to a combination of exponential functions or an appropriately selected polynomial function, and the first derivatives of the fitted curves were calculated at  $t = 0$ . The initial absorbance change is almost exclusively due to the formation of  $\text{ClO}_2$ , and the first derivative is proportional to the initial rate. It should be emphasized that the mathematical functions used in these calculations were not derived on the basis of any specific kinetic model and the parameters obtained from this fitting procedure cannot be assigned to any part of the mechanism.

The rate, defined as  $v = dA/dt$ , was very sensitive to the conditions applied at  $t = 0$ , and it decreased significantly in the first 50–100 ms of the reaction. Because the reactant concentrations changed only slightly within this time frame, the observations strongly suggest the contribution of more than one step to the overall redox process. These features of the reaction resulted in relatively large uncertainties in the estimated values of the initial rates ( $v_i$ ). Therefore, whenever it was feasible, the better defined derivatives of the kinetic traces at 25 ms were used as  $v_i$ .

At constant pH, the initial rate was proportional to either  $[\text{ClO}_2^-]$  or  $[\text{Br}_2]$  when the concentration of the other reactant was kept constant. It should be added that the experimentally accessible concentrations of bromine could be changed by only

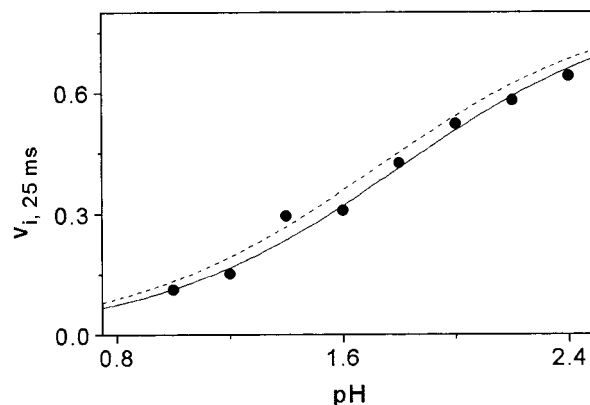


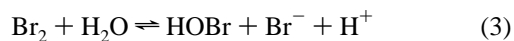
**Figure 2.** pH dependence of the initial rate of the bromine–chlorite ion reaction. Key: initial rates estimated on the basis of the experimental kinetic traces (●) and predicted by model C in Table 1 (dashed line); fit of the data to eq 6 (solid line).  $v_{i,25\text{ms}} = dA_{370\text{nm}}/dt$  at 25 ms, in  $\text{s}^{-1}$ ;  $[\text{ClO}_2^-]_0 = 5.0 \times 10^{-3} \text{ M}$ ;  $[\text{Br}_2]_0 = 5.0 \times 10^{-4} \text{ M}$ ;  $[\text{Br}^-] = 0.05 \text{ M}$ .

about a factor of 4. Despite the limitations, it could be shown that the initial reaction was roughly first order with respect to both  $[\text{ClO}_2^-]_{\text{tot}}$  and  $[\text{Br}_2]_{\text{tot}}$ . The corresponding rate law is given as

$$\left(-\frac{d[\text{Br}_2]}{dt}\right)_i = -\left(\frac{1}{2}\frac{d[\text{ClO}_2^-]}{dt}\right)_i = k_i[\text{Br}_2]_{\text{tot}}[\text{ClO}_2^-]_{\text{tot}} \quad (2)$$

Because of the hydrolysis of bromine and the protolytic equilibrium of chlorine(III), this simple rate law represents the combined effect of the parallel reactions of  $\text{Br}_2$  and  $\text{HOBr}$  with  $\text{HClO}_2$  and  $\text{ClO}_2^-$ . At pH 1.50, the estimated value for  $k_i$  is  $\sim 2700 \text{ M}^{-1} \text{ s}^{-1}$ .

**Effect of pH.** In the pH 1.00–8.00 region, the initial rate shows a maximum as a function of pH. For the interpretation of the results, the following fast preequilibria need to be considered:



In the slightly acidic–neutral pH range, chlorine(III) is present as  $\text{ClO}_2^-$ , while bromine undergoes hydrolysis and is converted to  $\text{BrO}^-$  when the pH is increased. The hypobromite ion is practically inert in the redox process, and the decreasing reaction rate correlates well with the deprotonation of  $\text{HOBr}$ . These findings confirm recent results reported by Furman and Margerum.<sup>14</sup> Under acidic conditions (pH < 3.0), reaction 4 is shifted to the right, and the pH dependence of the initial rate may indicate different reactivities between  $\text{HClO}_2$  and  $\text{ClO}_2^-$  and/or between  $\text{Br}_2$  and  $\text{HOBr}$ .

In the presence of excess  $\text{Br}^-$  and at pH < 3.0, the hydrolysis of  $\text{Br}_2$  is suppressed,  $\text{Br}_3^-$  is formed in significant amounts, and the  $[\text{Br}_2]/[\text{Br}_3^-]$  ratio is practically constant ( $\sim 1/1$  when  $[\text{Br}^-] = 0.05 \text{ M}$ ). Thus, any variation in the rate as a function of pH corresponds to the acid dissociation of chlorous acid. As indicated by Figure 2, only the  $\text{ClO}_2^-$  form of Cl(III) is reactive in the redox process and the initial rate should reach a limiting value when the deprotonation of  $\text{HClO}_2$  is completed by increasing the pH. On the basis of the above considerations,

(34) Valdes-Aguilera, O.; Boyd, D. W.; Epstein, I. R.; Kustin, K. *J. Phys. Chem.* **1986**, *90*, 6702–6708.



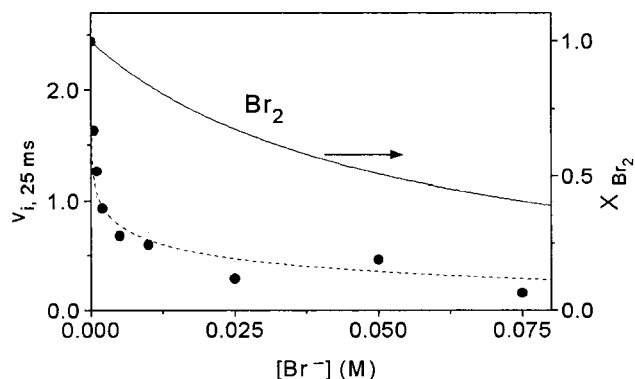


**Figure 3.** Initial rate and bromine concentration as functions of  $[\text{Br}^-]$ . Key: initial rates estimated on the basis of the experimental kinetic traces (●) and predicted by model C in Table 1 (dashed line);  $\text{Br}_2$  concentration expressed as the mole fraction of total bromine (solid line).  $v_{i,25\text{ms}} = dA_{370\text{nm}}/dt$  at 25 ms, in  $\text{s}^{-1}$ ;  $[\text{ClO}_2^-]_0 = 1.0 \times 10^{-2} \text{ M}$ ;  $[\text{Br}_2]_0 = 5.0 \times 10^{-4} \text{ M}$ ; pH = 1.50.

the pH dependence of the initial rate can be expressed as

$$v_i = v_{i,\text{lim}} \frac{1}{1 + K_p[\text{H}^+]} \quad (6)$$

where  $v_i$ ,  $v_{i,\text{lim}}$ , and  $K_p$  are the initial rate, the limiting initial rate characteristic for the  $\text{ClO}_2^-$  form of Cl(III), and the protonation constant of the chlorite ion, respectively. The protonation constant obtained by fitting the kinetic data,  $\log K_p = 1.80 \pm 0.04$ , agrees reasonably well with our value reported earlier,<sup>24</sup> 1.72. It should be noted that  $v_{i,\text{lim}}$  cannot be determined experimentally because the hydrolysis of  $\text{Br}_2$  interferes with the  $\text{ClO}_2^-$ – $\text{Br}_2$  reaction at higher pH, even in the excess of bromide ion.

**Bromide Ion Effect.** The bromide ion has a significant retarding effect on the reaction rate. To some extent, this is due to the conversion of  $\text{Br}_2$  into the unreactive  $\text{Br}_3^-$ . The initial rate is proportional to the free bromine concentration,  $[\text{Br}_2]$ , in a large excess of the bromide ion. However, a comparison of the reaction rate and the speciation as a function of  $[\text{Br}^-]$  reveals that the formation of the tribromide ion alone does not explain the noted inhibition. As shown in Figure 3, the initial rate decreases more sharply than  $[\text{Br}_2]$  at low  $[\text{Br}^-]$ . These observations strongly suggest that the bromide ion controls not only the  $[\text{Br}_2]/[\text{Br}_3^-]$  ratio but also the concentrations of HOBr and other reactive intermediates, such as  $\text{Br}_2^-$  and Br, which are presumably significant in the redox process.

The effect of the bromide ion on the HOBr–chlorite ion reaction was studied in separate experiments at pH 1.50. As expected, the initial rate gradually decreased when  $\text{Br}^-$  was added to the samples in increasing concentrations.

**Effect of Chlorine Dioxide.** In most kinetic runs, the absorbance changes became increasingly slower over the course of the reaction. This autoinhibitive feature of the kinetic traces was more pronounced when  $[\text{Br}^-]_0$  was increased. The inhibition is probably due to the formation of chlorine dioxide because this species is able to efficiently reduce the initial rate in the presence of excess  $\text{Br}^-$  (Figure 4). It was also confirmed that the apparent reaction order for  $[\text{ClO}_2^-]$  increased when chlorine dioxide was initially added to the reaction mixture.

In related experiments, we found that the initial rate was independent of  $[\text{ClO}_2^-]$  in the absence of added bromide ion. There is ample evidence in the literature that chlorine dioxide and the bromide ion coexist in aqueous solution and direct reaction does not occur between these species. Therefore, it must

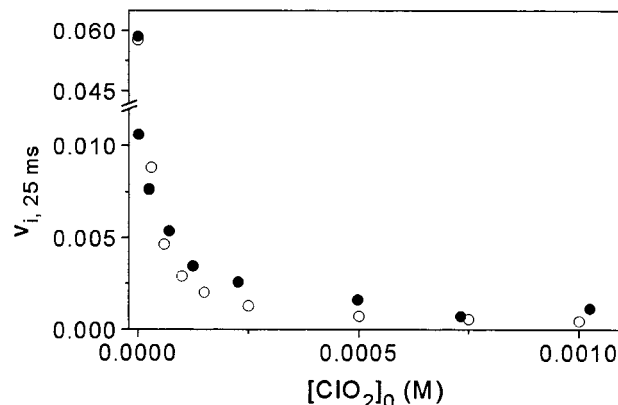


**Figure 4.** Initial rate as a function of added chlorine dioxide concentration. Key: initial rates estimated on the basis of the experimental kinetic traces (●) and predicted by model C in Table 1 (○).  $v_{i,25\text{ms}} = dA_{370\text{nm}}/dt$  at 25 ms, in  $\text{s}^{-1}$ ;  $[\text{ClO}_2^-]_0 = 1.0 \times 10^{-3} \text{ M}$ ;  $[\text{Br}_2]_0 = 5.0 \times 10^{-4} \text{ M}$ ;  $[\text{Br}^-] = 0.05 \text{ M}$ ; pH = 1.50.

be assumed that the inhibition involves the reaction of  $\text{ClO}_2$  with a reactive intermediate which may regenerate the chlorite ion. When  $[\text{Br}^-]$  is low, this step is inferior to the reaction path that leads to the completion of the overall process. According to these considerations,  $\text{Br}^-$  is not involved directly in the inhibition. To account for the  $[\text{Br}^-]$  dependence, we propose that the bromide ion increases the kinetic weight of the inhibition step by suppressing the competing reaction path.

**Detection of  $\text{BrClO}_2$ .** The formation of this intermediate was deduced from single-wavelength stopped-flow measurements by Valdes-Aguilera and co-workers.<sup>1</sup> It was assumed that the nonzero initial absorbance of the traces in the near UV–visible region was due to  $\text{BrClO}_2$ . The spectrum reported for this species was very similar to that of  $\text{ClO}_2$ . The maxima of the characteristic spectral bands occurred at the same wavelengths, though the transient species had a somewhat weaker absorbance.

Time-resolved spectra obtained in the present study are consistent with steady formation of  $\text{ClO}_2$ , and the extrapolated small absorbance values at  $t = 0$  can be interpreted by taking into account the colored bromine species. In the single-wavelength stopped-flow measurements, the variation of the initial absorbance as a function of  $[\text{Br}^-]$  could also be interpreted in terms of the  $\text{Br}_2$ – $\text{Br}_3^-$  equilibrium. Thus, the experimental data do not confirm the formation of any new absorbing species. The spectrum of  $\text{BrClO}_2$  reported previously should be termed an artifact probably due to the limitations of the equipment used in that early study. As will be discussed in detail, these findings do not exclude the possibility that  $\text{BrClO}_2$  is formed at low concentration levels and plays an important kinetic role in this system.

**The Kinetic Model.** The complex pH and concentration dependencies of the reaction rate require the use of a multistep kinetic model for the interpretation of the experimental data. Several models were tested by comparing experimental and simulated kinetic curves at 370 nm. In these calculations, the traces were truncated such that the second phase of the overall process, i.e., the relatively slow  $\text{Br}^-$ – $\text{ClO}_2^-$  reaction, could be omitted. In the absence and presence of added  $\text{Br}^-$ , the traces were used up to 90 and 60% conversion of  $\text{Br}_2$ , respectively. The kinetic model was represented by an appropriate differential equation system which was solved with the GEAR algorithm.<sup>28</sup> The absorbance–time profiles were calculated by using the following molar absorbances (in  $\text{M}^{-1} \text{ cm}^{-1}$ ):  $\text{ClO}_2$ , 962;  $\text{Br}_2$ , 133;  $\text{Br}_3^-$ , 545; HOBr, 12. These values were determined in separate experiments by recording the spectra of  $\text{ClO}_2$ ,  $\text{ClO}_2^-$

**Table 1.** Kinetic Models for Br<sub>2</sub> Oxidation of the Chlorite Ion

reaction	no.	log <i>K</i>	comment	rate const	rate const values <sup>a</sup>			comment
					model A	model B	model C	
Br <sub>2</sub> + ClO <sub>2</sub> <sup>-</sup> = ClO <sub>2</sub> + Br <sub>2</sub> <sup>-</sup>	R1	-5.93	<i>b</i>	<i>k</i> <sub>1</sub>	(4.3 ± 0.4) × 10 <sup>3</sup>	(1.7 ± 0.4) × 10 <sup>3</sup>	(1.3 ± 0.2) × 10 <sup>3</sup>	<i>c</i>
				<i>k</i> <sub>-1</sub>	3.7 × 10 <sup>9</sup>	1.5 × 10 <sup>9</sup>	1.1 × 10 <sup>9</sup>	<i>d</i>
Br <sub>2</sub> <sup>-</sup> + ClO <sub>2</sub> <sup>-</sup> = ClO <sub>2</sub> + 2Br <sup>-</sup>	R2	11.40	<i>b</i>	<i>k</i> <sub>2</sub>	(2.9 ± 0.1) × 10 <sup>6</sup>	(4.0 ± 0.1) × 10 <sup>6</sup>	(4.0 ± 0.1) × 10 <sup>6</sup>	<i>c</i>
				<i>k</i> <sub>-2</sub>	1.2 × 10 <sup>-5</sup>	1.6 × 10 <sup>-5</sup>	1.6 × 10 <sup>-5</sup>	<i>d</i>
Br <sub>2</sub> + Br <sup>-</sup> = Br <sub>3</sub> <sup>-</sup>	R3	1.28	<i>c</i>	<i>k</i> <sub>3</sub>	1.5 × 10 <sup>9</sup>	1.5 × 10 <sup>9</sup>	1.5 × 10 <sup>9</sup>	ref 36
				<i>k</i> <sub>-3</sub>	7.8 × 10 <sup>7</sup>	7.8 × 10 <sup>7</sup>	7.8 × 10 <sup>7</sup>	<i>d</i>
ClO <sub>2</sub> <sup>-</sup> + H <sup>+</sup> = HClO <sub>2</sub>	R4	1.72	ref 24	<i>k</i> <sub>4</sub>	1.0 × 10 <sup>10</sup>	1.0 × 10 <sup>10</sup>	1.0 × 10 <sup>10</sup>	<i>e</i>
				<i>k</i> <sub>-4</sub>	1.9 × 10 <sup>8</sup>	1.9 × 10 <sup>8</sup>	1.9 × 10 <sup>8</sup>	<i>d</i>
Br <sub>2</sub> = HOBr + Br <sup>-</sup> + H <sup>+</sup>	R5	-8.22	ref 35	<i>k</i> <sub>5</sub>	9.7 × 10	9.7 × 10	9.7 × 10	ref 35
				<i>k</i> <sub>-5</sub>	1.6 × 10 <sup>10</sup>	1.6 × 10 <sup>10</sup>	1.6 × 10 <sup>10</sup>	ref 35
Br + Br <sup>-</sup> = Br <sub>2</sub> <sup>-</sup>	R6	5.04	<i>b</i>	<i>k</i> <sub>6</sub>	(1.3 ± 0.1) × 10 <sup>10</sup>	1.0 × 10 <sup>10</sup>	1.0 × 10 <sup>10</sup>	<i>c</i>
				<i>k</i> <sub>-6</sub>	1.2 × 10 <sup>5</sup>	9.1 × 10 <sup>4</sup>	9.1 × 10 <sup>4</sup>	<i>d</i>
Br + Br = Br <sub>2</sub>	R7	27.35	<i>b</i>	<i>k</i> <sub>7</sub>	1.0 × 10 <sup>10</sup>	1.0 × 10 <sup>10</sup>	1.0 × 10 <sup>10</sup>	<i>e</i>
				<i>k</i> <sub>-7</sub>	4.5 × 10 <sup>-18</sup>	4.5 × 10 <sup>-18</sup>	4.5 × 10 <sup>-18</sup>	<i>d</i>
Br + ClO <sub>2</sub> <sup>-</sup> = ClO <sub>2</sub> + Br <sup>-</sup>	R8	16.37	<i>b</i>	<i>k</i> <sub>8</sub>	(5.4 ± 0.4) × 10 <sup>9</sup>		(2.3 ± 0.7) × 10 <sup>8</sup>	<i>c</i>
				<i>k</i> <sub>-8</sub>	2.3 × 10 <sup>-7</sup>		9.7 × 10 <sup>-9</sup>	<i>d</i>
HOBr + HClO <sub>2</sub> = BrClO <sub>2</sub> + H <sub>2</sub> O	R9	11.84	<i>f</i>	<i>k</i> <sub>9</sub>		(2.4 ± 0.1) × 10 <sup>5</sup>	(1.9 ± 0.1) × 10 <sup>5</sup>	<i>c, g</i>
				<i>k</i> <sub>-9</sub> / <i>K</i> <sub>10</sub>		3.5 × 10 <sup>-7</sup>	2.8 × 10 <sup>-7</sup>	<i>d</i>
BrClO <sub>2</sub> + ClO <sub>2</sub> <sup>-</sup> = 2ClO <sub>2</sub> + Br <sup>-</sup>	R10							

<sup>a</sup> The units for the first-, second-, and third-order rate constants are s<sup>-1</sup>, M<sup>-1</sup> s<sup>-1</sup>, and M<sup>-2</sup> s<sup>-1</sup>, respectively. <sup>b</sup> Calculated from the redox potentials listed in Table 2. <sup>c</sup> This work. <sup>d</sup> *k*<sub>-</sub> = *k*<sub>+</sub>/*K*. <sup>e</sup> Estimated value. <sup>f</sup> Overall equilibrium constant for R9 and R10. <sup>g</sup> On the basis of eq 10.

**Table 2.** Standard Redox Potentials of Redox Couples Formed in the Br<sub>2</sub>-ClO<sub>2</sub><sup>-</sup> Reaction

reaction	<i>E</i> <sup>o</sup> (V)	ref	reaction	<i>E</i> <sup>o</sup> (V)	ref
ClO <sub>2</sub> + e <sup>-</sup> ⇌ ClO <sub>2</sub> <sup>-</sup>	+0.936	37	1/2Br <sub>2</sub> + e <sup>-</sup> ⇌ Br <sup>-</sup>	+1.098	38
Br <sub>2</sub> + e <sup>-</sup> ⇌ Br <sub>2</sub> <sup>-</sup>	+0.58	37	Br + e <sup>-</sup> ⇌ Br <sup>-</sup>	+1.92	37
Br <sub>2</sub> <sup>-</sup> + e <sup>-</sup> ⇌ 2 Br <sup>-</sup>	+1.62	37			

solutions, and a series of Br<sub>2</sub>/Br<sub>3</sub><sup>-</sup> solutions in the stopped-flow instrument. It was assumed that the absorbance was a linear combination of the concentrations of the colored species, and the speciation in the samples was calculated on the basis of the equilibrium constants listed in Table 1. At 370 nm, only ClO<sub>2</sub>, Br<sub>3</sub><sup>-</sup>, and Br<sub>2</sub> have measurable contributions to the absorbance. The initial absorbance is determined by the two bromine species, and the absorbance of chlorine dioxide becomes dominant at longer reaction times.

The kinetic model postulates a series of reversible reaction steps (Table 1). The equilibrium constants for these reactions either were available from direct equilibrium studies,<sup>24,35</sup> for R4 and R5, or were calculated from the standard redox potentials of the redox couples listed in Table 2. The value of *K*<sub>R3</sub> was determined in the present study (see the Experimental Section). In the final calculations, the equilibrium constants were fixed at their known values. The reverse reaction steps were included by calculating their rate constants as the ratios of the corresponding forward rate constants and equilibrium constants. Kinetic traces obtained at various reactant concentrations and pHs (ca. 3800 data points in 11 curves) were fitted simultaneously, and the forward rate constants were estimated using a nonlinear least-squares algorithm.<sup>28</sup>

In the presence of excess bromide ion, a limited kinetic model using R1–R4 is sufficient to explain the observations. The initial electron transfer between Br<sub>2</sub> and ClO<sub>2</sub><sup>-</sup> is not favored thermodynamically, but the second step carries the reduction of bromine to completion. On the basis of earlier reports, the molar absorbance of Br<sub>2</sub><sup>-</sup> is about 9500 M<sup>-1</sup> cm<sup>-1</sup> at 370 nm.<sup>39,40</sup> Because this species is present at very low steady-state

concentrations, its contribution to the spectral effects is always negligible. The value of *k*<sub>3</sub> was known from earlier studies,<sup>36</sup> while the protolytic equilibrium between HClO<sub>2</sub> and ClO<sub>2</sub><sup>-</sup> was assumed to be diffusion controlled (*k*<sub>4</sub> = 1.0 × 10<sup>10</sup> M<sup>-1</sup> s<sup>-1</sup>). With these rate constants kept at fixed values, the calculations gave *k*<sub>1</sub> = (1.4 ± 0.3) × 10<sup>3</sup> M<sup>-1</sup> s<sup>-1</sup> and *k*<sub>2</sub> = (4.1 ± 0.1) × 10<sup>6</sup> M<sup>-1</sup> s<sup>-1</sup>.

The simplified model does not account for the noted [Br<sup>-</sup>] dependence of the reaction rate (Figure 3). Upon a decrease in the bromide ion concentration, the hydrolysis of bromine, R5, is shifted toward HOBr formation, and the Br<sub>2</sub><sup>-</sup> radical dissociates into Br<sup>-</sup> and Br in a reversible step, R6.<sup>39,40</sup> Both HOBr and Br are strong oxidants, which may open new reaction paths in the redox process. We included the corresponding steps in the kinetic model and tested how separate reactions of the chlorite ion with these oxidants would improve the overall fit of the data.

Model A (Table 1) implies that the R6, R8 sequence efficiently competes with R2. Step R7 is a dead end with respect to this path. However, Br is always present at very low concentration levels, and this radical–radical type of recombination is always inferior compared to R8. The [Br<sup>-</sup>] dependence of the overall rate can be explained by considering the competition between the forward steps of R6 and R8. In the absence of the bromide ion, Br may react exclusively with ClO<sub>2</sub><sup>-</sup>. When the concentration of Br<sup>-</sup> is increased, the recombination of Br<sub>2</sub><sup>-</sup>, R6, becomes faster and the steady-state concentration of the Br radical decreases. Consequently, the contribution of R8 to the oxidation process becomes negligible by increasing [Br<sup>-</sup>].

The agreement between experimental and calculated data was substantially improved when the Br path was included in the model. The results of the calculations are listed in Table 1. As expected, the model predicts that the Br radical is involved in extremely fast reactions. The value obtained for *k*<sub>6</sub> is consistent with the rough estimate, ~10<sup>10</sup> M<sup>-1</sup> s<sup>-1</sup>, derived for the same rate constant from pulse radiolytic experiments.<sup>39</sup> The reactions

(35) Beckwith, R. C.; Wang, T. X.; Margerum, D. W. *Inorg. Chem.* **1996**, *35*, 995–1000.

(36) Ruasse, M.; Aubard, J.; Galland, B.; Adenier, A. *J. Phys. Chem.* **1986**, *90*, 4382–4388.

(37) Stanbury, D. M. *Adv. Inorg. Chem.* **1989**, *33*, 69–138.

(38) Bratsch, S. G. *J. Phys. Ref. Data* **1989**, *18*, 1–21.

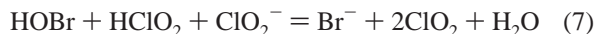
(39) Zehavi, D.; Rabani, J. *J. Phys. Chem.* **1972**, *76*, 312–319.

(40) Stevenson, K. L.; Knorr, D. W.; Horváth, A. *Inorg. Chem.* **1996**, *35*, 835–839.

of simple neutral radicals are expected to be diffusion controlled, and the value obtained for  $k_8$  seems to be acceptable also.

In model B, the bromide ion affects the reaction by controlling the concentration of HOBr via R5. In a recent study, the oxidation of  $\text{ClO}_2^-$  by HOBr was found to be first order with respect to both reactants.<sup>14</sup> The proposed mechanism postulates the formation of a weak adduct between the reactants,  $\text{HOBrOClO}^-$ , which is converted to  $\text{BrClO}_2$  in a subsequent acid-catalyzed step. The reaction is completed by fast reactions of the latter intermediate with  $\text{ClO}_2^-$  and  $\text{OH}^-$ . This mechanism is consistent with the experimental observations in the slightly acidic–neutral pH region.<sup>14</sup> When the  $\text{ClO}_2^-$ –HOBr reaction was incorporated into our model, the fit of the data did not improve because this step is too slow to affect the overall rate under the acidic conditions applied in the present study. However, an additional reaction path may exist between HOBr and the protonated form of chlorine(III). These considerations imply that the formation of  $\text{BrClO}_2$  is much faster from  $\text{HClO}_2$  than from  $\text{ClO}_2^-$ . It seems reasonable to assume that  $\text{BrClO}_2$  is extremely reactive and is present at very low steady-state concentrations. This would also explain why the formation of this species could not be detected experimentally.

The properties of the  $\text{BrClO}_2$  intermediate are not known in aqueous solution, and appropriate data are not available to estimate even the approximate magnitudes of the equilibrium and rate constants for R9 and R10. Only an overall equilibrium constant,  $K_{\text{R9,R10}} = 6.9 \times 10^{11}$ , can be calculated for the combination of the two steps



To include steps R9 and R10 in the model, a rate equation was derived for this sequence by using a steady-state approach for  $\text{BrClO}_2$ :

$$\frac{d[\text{HOBr}]}{dt} = \frac{-k_9 k_{10} [\text{HOBr}][\text{HClO}_2][\text{ClO}_2^-] + k_{-9} k_{-10} [\text{ClO}_2]_2 [\text{Br}^-]}{k_{-9} + k_{10} [\text{ClO}_2^-]} \quad (8)$$

While the reverse path of the R<sub>9</sub>, R<sub>10</sub> sequence is negligible, the reverse step of R9 can be fast. The concentration dependencies of the rate law are determined by the relative rate of this reaction compared to that of the forward step of R10. If R9 is a fast preequilibrium compared to R10, i.e.,  $k_{-9} \gg k_{10}[\text{ClO}_2^-]$ , the forward and reverse rates for the combined reaction can be given as

$$\begin{aligned} \nu_+ &= k_{10} K_9 [\text{HOBr}][\text{HClO}_2][\text{ClO}_2^-] \\ \nu_- &= k_{-10} [\text{ClO}_2]_2 [\text{Br}^-] \end{aligned} \quad (9)$$

Alternatively, if  $k_{-9} \ll k_{10}[\text{ClO}_2^-]$

$$\nu_+ = k_9 [\text{HOBr}][\text{HClO}_2] \quad \nu_- = \frac{k_{-9}}{K_{10}} \frac{[\text{ClO}_2]_2 [\text{Br}^-]}{[\text{ClO}_2^-]} \quad (10)$$

Both sets of rate expressions were used in the calculations by fitting  $k_1$ ,  $k_2$ , and  $k_{10}K_9$  or  $k_9$ . With eq 9, the fit was less satisfactory, and this option was rejected in further calculations. The results obtained with eq 10 are shown in Table 1 (model B).

The calculations confirm that the inclusion of the HOBr (by using eq 10) or the Br path leads to equivalent kinetic models. This strongly suggests that the pH and  $[\text{Br}^-]$  dependencies of the corresponding reaction rates are very similar. However, it is very likely that the oxidations of the chlorite ion by Br and by HOBr occur simultaneously and that the alternative models represent the limiting cases of the same mechanism. Therefore, we combined models A and B and attempted to fit all relevant kinetic data simultaneously. These calculations gave an unrealistically large value for  $k_6$ , indicating that the experimental data do not carry sufficient kinetic information for R6. When this rate constant was fixed at  $10^{10} \text{ M}^{-1} \text{ s}^{-1}$ ,  $k_1$ ,  $k_2$ ,  $k_8$ , and  $k_9$  could be estimated with reasonable precision (model C, Table 1). The values of the fitted rate constants changed by 25% at most ( $k_1$ ) when  $k_6$  was varied from  $5 \times 10^9$  to  $1.5 \times 10^{10} \text{ M}^{-1} \text{ s}^{-1}$ . This range was selected by considering an earlier estimate<sup>39</sup> for  $k_6$ . The calculations revealed that the oxidation of the chlorite ion by HOBr was superior to the Br path, although the latter process could not be completely neglected.

Available literature data for the individual reaction steps support the results presented here. The reverse rate constant obtained for R1 is in excellent agreement with the value reported earlier,<sup>41</sup>  $1.2 \times 10^9 \text{ M}^{-1} \text{ s}^{-1}$ . It follows that, in agreement with our results,  $k_1$  needs to be on the order of  $10^3 \text{ M}^{-1} \text{ s}^{-1}$ . This value is about 2 orders of magnitude larger than that predicted by the Marcus theory. Such deviations from the outer-sphere electron-transfer model were found in a few redox reactions between simple main-group compounds. It was proposed that some sort of overlap mechanism, which is very similar to the inner-sphere mechanism in coordination chemistry, is operative in these systems.<sup>42</sup>

On the basis of pulse radiolytic experiments at pH 6.7, a value,  $2.0 \times 10^7 \text{ M}^{-1} \text{ s}^{-1}$ , ~5 times larger than that obtained here was reported for  $k_2$ .<sup>43</sup> Although the experimental details are not given in that paper, it is very likely that a great part of the noted deviation is due to the differences in the experimental conditions and methods. The results are consistent in that the rate of R2 is far below the diffusion-controlled limit. Electrostatic repulsion between the uniformly charged reactants may somewhat retard this step, but other factors must have a more significant effect on the reaction rate. For example, the dissociation of the Br–Br bond of  $\text{Br}_2^-$  may hinder the electron-transfer process.

To test the validity of the proposed model, the concentration dependencies of the initial rate were calculated for the conditions shown in Figures 2–4. The model predicts the same trends as observed experimentally though there are deviations between the  $\nu_i$  values obtained from the experimental kinetic traces and those calculated on the basis of the model. This reflects the noted uncertainties associated with the estimation of  $\nu_i$ . Direct comparison of the experimental and calculated kinetic curves offers a better way to validate the model. In this case, approximations are not involved and entire kinetic profiles are compared. The reasonably good agreement between measured and calculated traces (Figure 5) is a clear indication that the proposed model gives a proper interpretation of the kinetic features of the  $\text{Br}_2^-$ – $\text{ClO}_2^-$  reaction under the conditions studied.

Recently, some arguments regarding the aqueous-phase structure of  $\text{BrClO}_2$  were presented by Furman and Margerum.<sup>14</sup>

(41) Mialocq, J. C.; Barat, F.; Gilles, L.; Hickel, B.; Lesigne, B. *J. Phys. Chem.* **1973**, *77*, 742–749.

(42) Stanbury, D. M.; Martinez, R.; Tseng, E.; Miller, C. E. *Inorg. Chem.* **1988**, *27*, 4277–4280.

(43) Huie, R. E.; Neta, P. *J. Phys. Chem.* **1986**, *90*, 1193–1198.

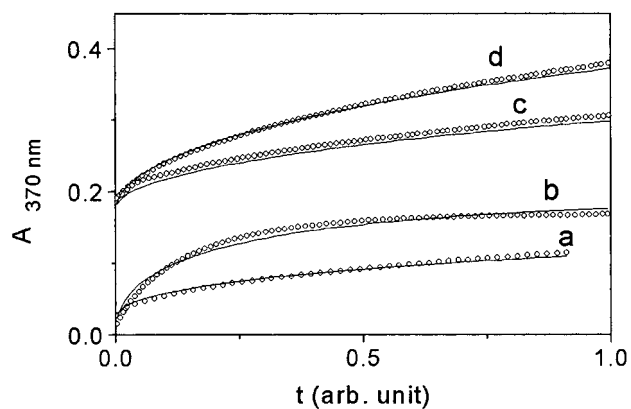
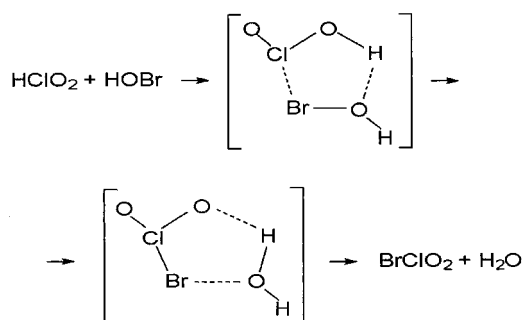


**Figure 5.** Experimental (open circles) and fitted (solid lines) kinetic traces for the bromine–chlorite ion reaction. The fitted traces were calculated on the basis of model C in Table 1. a:  $[\text{ClO}_2^-]_0 = 3.0 \times 10^{-3}$  M,  $[\text{Br}_2]_0 = 1.0 \times 10^{-4}$  M,  $[\text{Br}^-] = 0.025$  M, pH = 1.50 (unit time: 10 s). b:  $[\text{ClO}_2^-]_0 = 7.5 \times 10^{-3}$  M,  $[\text{Br}_2]_0 = 1.0 \times 10^{-4}$  M, pH = 1.50 (2 s). c:  $[\text{ClO}_2^-]_0 = 5.0 \times 10^{-3}$  M,  $[\text{Br}_2]_0 = 5.0 \times 10^{-4}$  M,  $[\text{Br}^-] = 0.05$  M, pH = 1.40 (2 s). d:  $[\text{ClO}_2^-]_0 = 5.0 \times 10^{-3}$  M,  $[\text{Br}_2]_0 = 5.0 \times 10^{-4}$  M,  $[\text{Br}^-] = 0.05$  M, pH = 1.80 (2 s).

We agree with these authors that to outline the exact connectivity of the atoms is an elusive goal and that only indirect information is available to deduce the properties of this species. Our calculations confirmed that protonation of the chlorite ion promotes the formation of  $\text{BrClO}_2$ . However, this effect cannot be explained by the concept of general-acid catalysis proposed by Furman and Margerum.<sup>14</sup> Their kinetic data were obtained from the pH 4.5–9.5 region, where  $\text{HClO}_2$  is a minor species and its reactions could be neglected. In that mechanism, the acid-assisted step was necessary to explain how the precursor complex of the reactants was transformed into  $\text{BrClO}_2$ . However, a mechanistic changeover may occur in the reaction when the pH is decreased. In acidic solution, chlorous acid is a major species which can open a direct path to the formation of  $\text{BrClO}_2$ . We propose that  $\text{HClO}_2$  and  $\text{HOBr}$  form a precursor complex that is stabilized by a hydrogen bond and a halogen–halogen bond, as shown in Scheme 1. Thus,  $\text{BrClO}_2$  may form via fast rearrangement of the adduct and subsequent elimination of a water molecule. On the basis of pressure-dependent studies, the formation of a very similar precursor complex was suggested to occur in the initial phase of the  $\text{BrO}_3^- - \text{I}^-$  reaction.<sup>44</sup> In the model proposed here, the protonation of  $\text{ClO}_2^-$  is a fast

**Scheme 1**



preequilibrium which precedes the rate-determining step. According to Scheme 1,  $\text{BrClO}_2$  most likely has a Y structure in which the bromine and the two oxygen atoms are connected to the central Cl atom. Nevertheless, other mechanisms leading to other connectivities, for example, to  $\text{Br}-\text{O}-\text{Cl}-\text{O}$ , cannot be excluded.

In summary, the results presented here confirm that, under acidic conditions, the oxidation of the chlorite ion occurs in competing parallel redox steps in the  $\text{Br}_2 - \text{ClO}_2^-$  reaction. The concentration ratios of the oxidants,  $\text{Br}_2^-$ ,  $\text{Br}$ , and  $\text{HOBr}$ , formed after the initiation step, as well as the relative rates of the parallel reactions, are controlled by the bromide ion concentration and pH. The proposed model may lead to a better understanding of the mechanistic details of complex reactive systems that contain bromine and the chlorite ion.

**Acknowledgment.** We are indebted to Prof. Gilbert Gordon for helpful discussions. This work was supported by NATO Linkage Grant CRG.LG 973337 and by Grants OTKA T 029568 and M 028244 from the Hungarian National Research Foundation.

**Supporting Information Available:** A textual description of preliminary studies on the  $\text{HOBr}$ –chlorite ion reaction under acidic conditions and figures showing time-resolved spectral changes in the presence of added bromide ion, initial rate as a function of  $[\text{ClO}_2^-]$  in the absence and presence of added  $\text{ClO}_2$  and  $\text{Br}^-$ , pH dependence of the initial rate in the pH 1.0–8.0 range, effect of the bromide ion on the initial rate of the  $\text{HOBr}$ –chlorite ion reaction, time-resolved rapid-scan spectra recorded in the first 130 ms of the reaction, and forward and reverse rates of the redox steps proposed in model C as a function of time in the absence and presence of added bromide ion. This material is available free of charge via the Internet at <http://pubs.acs.org>.

(44) Fábíán, I.; van Eldik, R. *Int. J. Chem. Kinet.* **1995**, *27*, 491–498.